ACS APPLIED MATERIALS & INTERFACES

Research Article

www.acsami.org

Development of Abamectin Loaded Plant Virus Nanoparticles for Efficacious Plant Parasitic Nematode Control

Jing Cao,[†] Richard H. Guenther,[‡] Tim L. Sit,[‡] Steven A. Lommel,[‡] Charles H. Opperman,[‡] and Julie A. Willoughby*[,†]

[†]Department of Textile Engineering, Chemistry and Science, North Carolina State University, 2401 Research Drive, Raleigh, North Carolina 27695, United States

[‡]Department of Plant Pathology, North Carolina State University, 850 Main Campus Drive, Raleigh, North Carolina 27695, United States

Supporting Information

ABSTRACT: Plant parasitic nematodes are one of the world's major agricultural pests, causing in excess of $157 billion in worldwide crop damage annually. Abamectin (Abm) is a biological pesticide with a strong activity against a wide variety of plant parasitic nematodes. However, Abm's poor mobility in the soil compromises its nematicide performance because of the limited zone of protection surrounding the growing root system of the plant. In this study, we manipulated Abm's soil physical chemistry by encapsulating Abm within the *Red clover necrotic mosaic virus* (RCNMV) to produce a plant virus nanoparticle (PVN) delivery system for Abm. The transmission electron microscopic and dynamic light scattering characterization of Abm-loaded PVN (PVN^{Abm}) indicated the resultant viral capsid integrity and morphology comparable to native RCNMV. In addition, the PVN^{Abm} significantly increased Abm's soil mobility while enabling a controlled release strategy for Abm's bioavailability to nematodes. As a result, PVN^{Abm} enlarged the zone of protection from *Meloidogyne hapla* root knot nematodes in the soil as compared to treating with free Abm molecules. Tomato seedlings treated with PVN^{Abm} had healthier root growth and a reduction in root galling demonstrating the success of this delivery system for the increased efficacy of Abm to control nematode damage in crops.

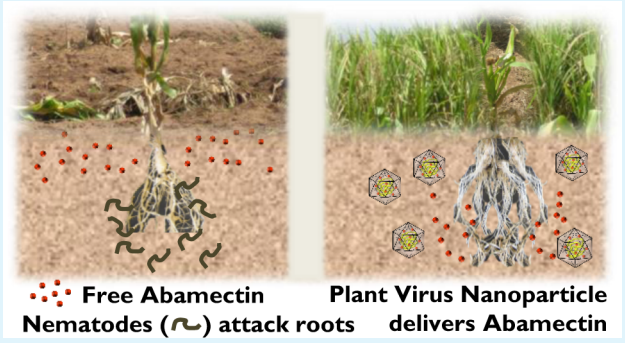

KEYWORDS: *red clover necrotic mosaic virus (RCNMV), plant virus nanoparticle (PVN), abamectin, soil mobility, crop protection*

1. INTRODUCTION

Plant parasitic nematodes (PPNs) are one of the world's major agricultural pests. Nematode infestation of cash crops will cause an excess of $157 billion in worldwide crop damage annually, further straining global food security.[1] As these parasitic worms attack crop root systems, they siphon crucial growth nutrients reducing crop yields. The surviving plants also are more vulnerable to secondary infections, drought, and other stresses. The vast majority of PPN damage is caused by sedentary endoparasitic forms, in particular, the root-knot (*Meloidogyne spp.*), soybean cyst (*Heterodera glycines*), and potato cyst (*Globodera spp.*) nematodes, which impact a wide range of crops, such as soybeans, potatoes, bananas, cotton, corn, strawberries, and tomatoes.[2] However, relatively few measures exist for controlling PPN infestation despite their large damage potential. Crop rotation is a commonly employed tactic to manage specific PPN species,[3] but its overall effectiveness is hampered by the polyspecific nature of most PPN infestations and may not be economically feasible for many growers. Host resistance is an environmentally and economically sound method to manage selected PPN species, but unfortunately, genetic resistance to PPNs is not available for most cultivated crops.[4] In addition, traditional methods for plant breeding require 5−10 years to produce a viable variety, however, new nematode control tools are an immediate and critical need. Although these PPN control strategies were reported to reduce nematode infection to some extent, none of them provided the same efficacious and economic benefits as the chemical treatment by nematicides.[5] It is estimated that the current market for nematicides is between $700 million and $1 billion annually worldwide.[6] An analysis of the economic impact of nematodes and growers' decision-making indicates that the nematicide market could grow to over $3 billion annually in the near future if effective and safe alternatives for treatment existed.[7]

Traditionally, one of the most effective pesticides for PPN control is dependent on highly toxic contact and fumigant nematicides, such as methyl bromide.[8] However, the use of

Received: February 2, 2015
Accepted: April 23, 2015
Published: April 23, 2015

DOI: 10.1021/acsami.5b00940
ACS Appl. Mater. Interfaces 2015, 7, 9546−9553

Scheme 1. Infusion of Small Molecules into RCNMV Capsid and Chemical Structure of Neutrally Charged Abamectin That Can Be Infused into PVN via the Described Infusion Procedures[a]

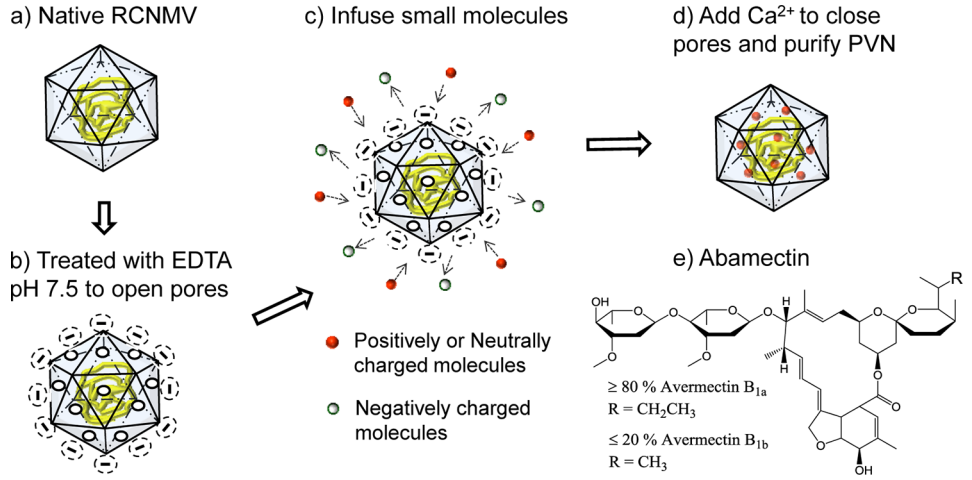

[a]Infusion procedures: (a) Purifying native RCNMV, (b) treating RCNMV in EDTA at pH 7.5 buffer to induce highly negatively charged RCNMV capsid with open pores on its exterior surface, (c) electrostatically attracting positively or neutrally charged molecules to infuse through the open pores into RCNMV capsid but repelling negative charged molecules away from RCNMV capsid, and (d) adding Ca^{2+} to close the pores and purifying cargo-loaded RCNMV that is named as plant virus nanoparticle (PVN). Panel e shows chemical structure of neutrally charged abamectin.

these types of pesticides have been restricted or eliminated because of environmental concerns. Another option is the application of nonfumigant nematicides, but their repetitive use in crops leads to a loss of efficacy caused by soil microorganisms developing a resistance to them.[9] A biologically active ingredient, abamectin (Abm), is a promising nematicide for PPN control. It is commercially available as a granular or liquid formulation (Avid) and most recently formulated as a seed coating (Avicta) by Syngenta Crop Protection. Abm is a mixture of macrocyclic lactone metabolites (≥80% avermectin B_{1a} and ≤20% avermectin B_{1b}) derived from the bacterium *Streptomyces avermitilis*.[10] Abm has been shown to have strong activity against a broad spectrum of nematodes yet is generally regarded as safe for mammals because of its inability to pass the blood-brain barrier.[10] Abm acts as a PPN control method through direct protein inhibition by binding to the glutamate receptors in nerve and muscle cells.[11] However, one basic problem that compromises Abm's efficacy is its insolubility in water and its lipophilic nature; hence, a high tendency to bind to organic contents in soil and poor distribution throughout the soil.[12−14] These traits create a very limited zone of protection around the developing root system. It has been reported that a large portion of the Abm dose remains with the seed coat, leaving the seedling radicle unprotected after germination.[15] Abm in liquid formulations also demonstrated minimal uptake by the root system with resultant poor efficacy.[16] Another drawback of Abm as a PPN nematicide is its lack of persistence over time because of its rapid degradation by photo-oxidation.[17] As a result, although PPN damage reduction is reported by using Abm formulations, it is generally minor (±50%) and only marginally economic for lower value crops. Therefore, there is a critical need to resolve the soil immobility issues for Abm compounds to enhance its effectiveness against PPN damage.

In this study, we developed an approach to increase the mobility or distribution of Abm within the soil by encapsulating it into a *red clover necrotic mosaic virus* (RCNMV)-derived plant virus nanoparticle (PVN). Use of a carrier, like RCNMV, could also improve Abm's stability against oxidation as well as isolate the toxicity of the nematicide from the end-user. Microencapsulation of Abm into a porous matrix has been developed by other researchers using different polymeric materials such as ethyl-cellulose,[18] zein,[19] and polyurea.[20] However, none of these Abm-microcapsules were evaluated for PPN control. The effect of organic solvents on Abm's bioactivity during polymerization is also unknown. To our knowledge, this is the first study to encapsulate Abm into nanoparticles for evaluation with a specific application. RCNMV is a $T = 3$ icosahedral soil-transmitted plant virus with a diameter of 36 nm.[21] The RCNMV capsid consists of 180 copies of the 37 kDa capsid protein (CP) that assembles to package the viral genome against the harsh environment in soils, demonstrating a robust structure for Abm encapsulation in agricultural application. Additionally, the RCNMV genomic RNAs and a portion of the CP subunits are self-organized to form a dodecadedral cage with a diameter of 17 nm within the RCNMV capsid.[22] This inner cage provides a nanoscale space for encapsulating foreign active cargo. The loading mechanism of RCNMV is controlled by (1) the electrostatic interactions between loading cargo and negatively charged RCNMV capsid and (2) the formation of open pores on RCNMV capsid surface.[22,23] In high concentrations (mM) of Ca^{2+} and Mg^{2+}, the RCNMV capsid remains in a hardy, closed form and able to withstand extremes of temperature, pH, and organic solvents. However, the RCNMV capsid undergoes a significant conformation change to form 90 pores (11−13 Å in diameter) on the capsid surface at low concentrations (nM) of Ca^{2+} and Mg^{2+}. This inherent behavior of RCNMV has been exploited for the intracellular delivery of chemotherapeutic drugs where the Ca^{2+} and Mg^{2+} concentration levels are in the nM range.[24] To create this condition in vitro, the addition of the ethylene diamine tetraacetic acid (EDTA) chelating agent at high pH value (>pH 7) is necessary.[23] These open pores provide channels for infusing small molecules into the RCNMV capsid. Using these features, as illustrated in Scheme 1, positively charged and neutrally charged cargoes, like rhodamine dye, luminarosine dye, and a chemotherapeutic drug doxorubicin (Dox), have been successfully infused into the RCNMV capsid in previous studies.[25,26] The cargo-loaded RCNMV is named as PVN^A

DOI: 10.1021/acsami.5b00940
ACS Appl. Mater. Interfaces 2015, 7, 9546−9553

where A is the loading cargo. For example, PVN^{Dox} formulated to target breast cancer cells demonstrated a great advantage for therapeutic drug delivery.[27,28] In addition to medical applications, RCNMV's inherent structural features, especially its robustness in soil, makes PVN an excellent carrier candidate for the delivery of Abm nematicide for PPN control in crop protection. The specific aims of this study were to (1) formulate PVN with Abm as a loading compound (PVN^{Abm}), (2) determine bioavailability of PVN^{Abm} to nematodes as compared to free Abm, and (3) evaluate the soil mobility of PVN^{Abm} and its crop protection for tomato seedlings in PPN infected soils.

2. MATERIALS AND METHODS

2.1. Materials. Abm powder was purchased from Sigma-Aldrich and dissolved in 90% (v v^{-1}) ethyl alcohol to make a stock solution at 2 mg mL^{-1}. Monobasic sodium phosphate, dibasic sodium phosphate, calcium chloride and sodium dodecyl sulfate (SDS) were obtained from Fisher Scientific. Ethylenediaminetetraacetic acid (EDTA) and sodium acetate was purchased from EMD Millipore. Proteinase K buffered aqueous glycerol solution, rhodamine, *N*-methylimidazole, trifluoroacetic anhydride, M9 buffer, and acetonitrile anhydrous was obtained from Sigma-Aldrich. Uranyl acetate was purchased from Electron Microscopy Sciences. All chemicals were used as received.

2.2. RCNMV Propagation and Purification. *Nicotiana clevelandii* plants (4−6 weeks old) were rub-inoculated with RCNMV RNA transcripts[29] and maintained in a greenhouse at 20−24 °C. After 7−10 days of propagation, the infected leaves were harvested and the virions were purified as previously described.[25] The concentration of virus was determined by absorbance measurement at 260 nm with an extinction coefficient (1 cm light path) of 6.46.[22] A pure virus preparation was determined by an A260 nm: A280 nm absorbance ratio of 1.63−1.69. The typical yield was approximately 8−20 mg of pure RCNMV from 100 g of infected leaf tissue. Native RCNMV was stored in 20 mM sodium phosphate buffer pH 7.2 at 4 °C before use to preserve its integrity over an extended period of 6 months.

2.3. Infusion of Abm into RCNMV Capsid. The protocol to load Abm within RCNMV capsid is illustrated in Scheme 1. RCNMV suspensions at a concentration of 6.43 mg mL^{-1} were pretreated in 20 mM sodium phosphate buffer pH 7.5 with 20 mM EDTA for 1 h to induce the pore-open condition on the exterior of the virus capsid. Next, a 2 mg mL^{-1} Abm solution was added at a molar ratio of 510:1 Abm to virion (the molecular weight of RCNMV is 1×10^7 g mol^{-1}) and then gently mixed overnight to allow the complete infusion of Abm. At the end of the infusion period, the viral capsid pores were closed by (i) the addition of 25 mM $CaCl_2$, (ii) lowering the solution pH with 0.2 M sodium acetate buffer pH 5.2, and (iii) incubation for an additional 30 min. Excess unincorporated Abm molecules were removed by running the loaded RCNMV through a size exclusion column (NAP 10 columns, GE Healthcare), and Abm-loaded RCNMV, named as PVN^{Abm}, were collected in 0.2 M sodium acetate buffer pH 5.2. PVN^{Abm} were formulated without EDTA treatment to validate the surface-bound Abm.[23] PVNs were also dually formulated with Abm and fluorescent dye rhodamine ($PVN^{Rho/Abm}$) to allow for tracking of PVNs in the mobility testing.

2.4. Physical Characterization of PVN^{Abm}. The morphology of native RCNMV and PVN^{Abm} was analyzed using transmission electron microscopy (JEOL 100S TEM) with negative staining. A 5 μL sample (~1 mg mL^{-1}) was deposited onto a copper mesh grid (Formvar/Carbon 400 mesh Cu grid, Ted Pella, Inc.) and wicked off after a 20 s immersion using Whatman filter paper. A 10 μL drop of 2% uranyl acetate solution (w v^{-1}) was applied and removed after 20 s. The prepared grid was vacuum-dried for 30 min and stored in a desiccation chamber before TEM observations.

Hydrodynamic diameter (d_H) of native RCNMV and PVN^{Abm} was measured in sodium acetate buffer pH 5.2 via dynamic light scattering using a Zetasizer Nano ZS instrument (Malvern Instruments). The measurements were conducted in a 4.5 mL disposable cuvette, where the Brownian motion of molecules in solution were detected by the fluctuations of the scattering intensity and then correlated to hydrodynamic size via the Stokes−Einstein equation.[30] The PVN concentration was 0.2 mg mL^{-1} for all measurements.

2.5. Quantitation of Abm in PVN^{Abm} by HPLC. *Derivatization Reaction.* PVN^{Abm} was disassociated with 2 mg mL^{-1} proteinase K and 2% (w v^{-1}) SDS solution to release all loaded Abm. Subsequently, an 80 μL aliquot of disassociated PVN^{Abm} mixture and standard Abm solutions at concentrations of 100, 40, 20, 10, and 2 μg mL^{-1} were dried under vacuum for 1 h until all liquid was evaporated. The dry residues were dissolved in 80 μL of anhydrous acetonitrile (ACN) and then mixed with 200 μL of *N*-methylimidazole solution in ACN (1:1, v/v). To initiate the derivatization reaction, 200 μL of trifluoroacetic anhydride solution in ACN (1:1, v/v) was added. After 1 min vortex mixing, a 10 μL aliquot of glacial acetic acid was added into the mixture and then placed in a 55 °C water bath for 30 min. The native RCNMV was also disassociated and derivatized as a negative control to test if it interfered with the HPLC assay. All derivatized solutions were transferred to the 2 mL autosampler vials (Agilent Technologies) for HPLC analysis.

HPLC Procedures and Loading Properties of PVN^{Abm}. The HPLC system consisted of an Infinity model 1260 HPLC pump (Model G1312B, Agilent Technologies), a standard autosampler (Model G1329B, Agilent Technologies) and a fluorescence detector (Model G1321B, Agilent Technologies). The separation was carried out on Agilent Poroshell 120 EC-C18 column (3.0 mm × 100 mm, 2.7 μm particle size) at a temperature of 40 °C. The mobile phase was 95% ACN (v v^{-1}) at a flow rate of 1.00 mL min^{-1}, and the injection volume of sample was 5 μL. The fluorescence detection was set to monitor an excitation wavelength of 365 nm and an emission wavelength of 470 nm. HPLC analysis was conducted within 6 h to avoid the degradation of the Abm derivatives. The peak areas were plotted against the Abm standard concentrations to establish the calibration curve using the least-squares linear regression analysis in OriginPro 8.5 data processing software (OriginLab). The amount of loaded Abm in each PVN^{Abm} formulation was calculated based on the standard calibration curve, while the concentration of PVN^{Abm} was measured with a NanoDrop 1000 Spectrophotometer at 260 nm with an extinction coefficient (1 cm light path) of 6.46. The loading capacity of PVN^{Abm} is reported as the number of Abm molecules associated with each viral capsid, and the loading efficiency is defined as the percentage of the Abm loaded with respect to the initial amount of Abm added to the loading preparation. Both parameters were calculated as

$$\text{loading capacity} = (\text{weight}_{\text{Abm loaded}}/\text{weight}_{\text{PVN}}) \times (\text{mw}_{\text{PVN}}/\text{mw}_{\text{Abm}}) \quad (1)$$

$$\text{loading efficiency} = (\text{weight}_{\text{Abm loaded}}/\text{weight}_{\text{total of added Abm}}) \times 100\% \quad (2)$$

where mw_{PVN} and mw_{Abm} are the molecular weights of PVN (1×10^7 g mol^{-1}) and Abm (837.11 g mol^{-1}), respectively.

2.6. In vitro Release Profiles of PVN^{Abm}. A dialysis-based assay was carried out to study the in vitro release of Abm molecules from PVN^{Abm}. A 180 μL aliquot of PVN^{Abm} suspension or free Abm solution at equivalent concentrations was injected into a dialysis bag with a MWCO of 3.5 kDa (Spectra/Por, Spectrum Laboratories, Inc.). The dialysis bag was immersed in 10 mL release medium containing either sodium acetate buffer (20 mM, pH 5.2) or M9 buffer (pH 7.4). At set intervals, the PVN^{Abm} suspension or free Abm solution were sampled from the dialysis bag and the concentration of remaining Abm was determined by the derivatization HPLC method as described above. Fresh release medium was replaced at every interval to maintain a constant sink condition. The release of PVN^{Abm} sample was run in triplicate. The capsid integrity of released PVN^{Abm} at different time points was measured by agarose gel electrophoresis.

2.7. Soil Mobility of $PVN^{Abm/Rho}$ and Free Abm/Rho. $PVN^{Abm/Rho}$, dually formulated with Abm and Rho fluorescence dye, was used to allow for tracking the fraction of PVN throughout the soil

DOI: 10.1021/acsami.5b00940
ACS Appl. Mater. Interfaces 2015, 7, 9546−9553

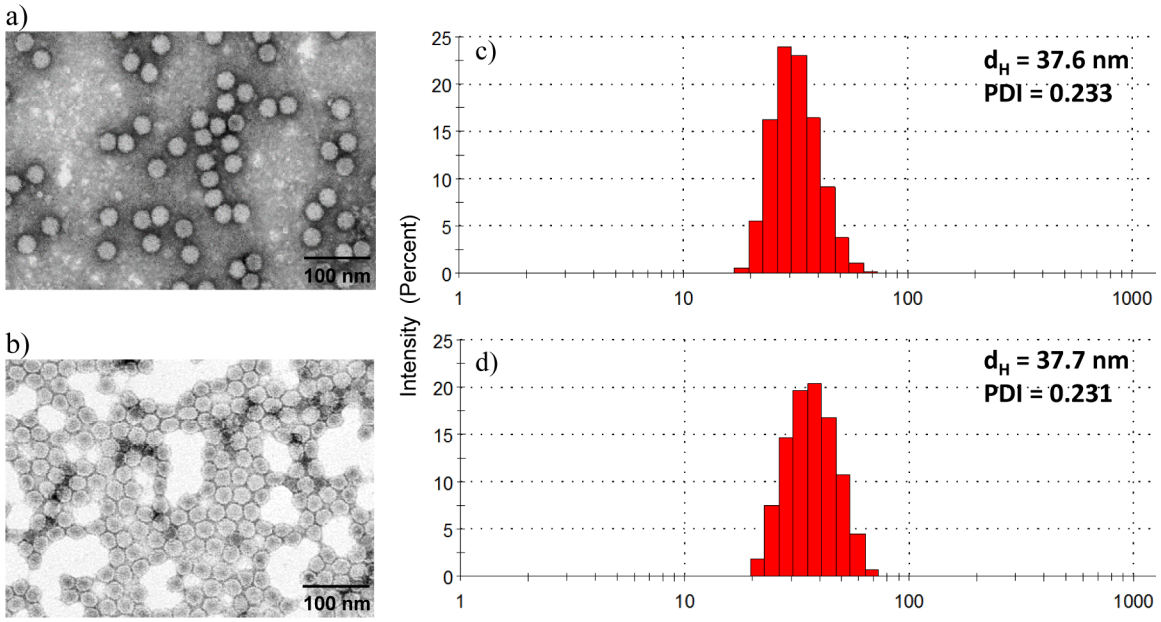

Figure 1. Characterization of native RCNMV and corresponding plant virus nanoparticle (PVN) via transmission electron microscopy for (a) RCNMV prior to loading and (b) after loading with Abm (PVN^{Abm}). Size distribution as measured by dynamic light scattering for hydrodynamic diameter (d_H) and polydispersity index (PDI) of (c) RCNMV and (d) PVN^{Abm}. * All RCNMV and PVN^{Abm} samples were measured in sodium acetate buffer pH 5.2.

via fluorescent detection. The soil mobility test was designed based on an Organization for Economic Cooperation and Development (OECD) detection method for identifying leaching in a soil column.[31] Briefly, two soil types (sandy loam soil and potting soil) were packed individually in a plastic column to a height of 4 cm. Subsequently, the soil was saturated with 5 mL deionized (DI) water. A 300 μL aliquot of $PVN^{Abm/Rho}$ or Abm/Rho mixture was applied on the top of the soil columns. Next, 24 aliquots of 300 μL DI water were added to elute through the soil column and collected individually in a well of a 24-well culture plate. Each collected fraction was assayed for the presence of active ingredient by measuring (1) fluorescence of Rho at the excitation wavelength of 530 nm and emission wavelength of 590 nm and (2) bioavailability of Abm to *Caenorhabditis elegans* (*C. elegans*) nematodes as described below.

2.8. Bioavailability of PVN^{Abm} to *C. elegans* Nematodes. The bioavailability of PVN^{Abm} and free Abm was assayed utilizing the model nematode *C. elegans* in liquid culture as described previously.[32] Briefly, a 5 μL aliquot of PVN^{Abm} with the Abm concentrations (1.8, 0.60, 0.20, 0.07 μg mL^{-1}), and free Abm at equivalent concentrations were added to each well of a 24-well culture plate, which was subsequently loaded with *C. elegans* nematodes (~50 individuals/well) cultured in 495 μL of M9 buffer. After 24 h incubation at room temperature, the nematodes in each treatment were evaluated on three scales: (1) totally immobilized determined as the loss of mobility and characteristic of a rigid, linear appearance, (2) impaired at 50% immobilized/50% mobilized, and (3) totally mobilized exhibiting flexible form and undulating movement. The lethal concentration 50 (LC_{50}) values, representing 50% immobilized nematodes at a given concentration of Abm, were reported for free Abm solution and PVN^{Abm} suspension.

2.9. Crop Protection of PVN^{Abm} to Plant Parasitic Nematode-Infected Tomato Seedlings. PVN^{Abm} and free Abm were applied to test the prevention of plant parasitic root knot nematode (RKN) *Meloidogyne hapla* (*M. hapla*) infection of tomato seedlings in 6-ounce foam cups under greenhouse conditions. The cups were filled with sandy loam soil and prewetted prior to transplanting. Two-week-old tomato seedlings that had uniform growth were selected for planting in the soil-filled cups and dosed with RKN inoculum (5000 eggs in 1 mL per cup) through three holes surrounding the root. Next, a total amount of 0.8 mg Abm in PVN^{Abm} suspension or free Abm solution was applied in each plant. Healthy plants without infection were taken as the negative control. The RKN-infected plants without Abm treatment were taken as the positive control. Each treatment was run in five replications, and the plants were watered as needed in the greenhouse. After 5 weeks of RKN inoculation, the roots of plants were harvested and gently washed with tap water. The galling on the root and the growth of the root were evaluated in each treatment to determine the efficacy of crop protection.

3. RESULTS AND DISCUSSION

3.1. Formulation and Characterization of PVN^{Abm}. RCNMV's unique response to divalent cation depletion and readdition enabled positively charged or neutrally charged small molecules to infuse into the viral capsid through a pore formation mechanism.[22−24] Using this feature, RCNMV has been developed as a nanovessel to carry the chemotherapeutic drug doxorubicin to fight against cancer.[25−28] In this study, we explored the use of RCNMV as a nanocarrier to enable efficacious delivery and tunable release of nematicides for PPN control in an agricultural application. Neutrally charged Abm molecules were loaded into RCNMV capsids to make the PVN^{Abm} formulation by inducing the pore-open condition of viral capsid (see Scheme 1). TEM image of PVN^{Abm} displayed the intact geometry of viral capsid after infusion with Abm. The surface morphology of PVN^{Abm} showed a similar pattern as native RCNMV where negatively stained protrusions were apparent on its outer surface (Figure 1a and 1b). The DLS hydrodynamic diameter (d_H) of PVN^{Abm} was measured as 37.6 nm with the polydispersity index (PDI) of 0.23 (Figure 1c), a value that is within the standard deviation of the DLS results for native RCNMV (d_H = 37.7, PDI = 0.231) (Figure 1d). Therefore, we conclude that the infusion of Abm did not cause a detectable change in the viral capsid properties of RCNMV.

To quantitatively determine the amount of Abm infused in the viral capsid, PVN^{Abm} was disassociated by proteinase digestion to release all loaded Abm. According to the methodology outlined by Payne et al.,[33] the disassociated mixture was subjected to a derivatization reaction to dehydrate

DOI: 10.1021/acsami.5b00940
ACS Appl. Mater. Interfaces 2015, 7, 9546−9553

the dihydroxycyclohexane ring of Abm to form an aromatic fluorescent moiety.[34] The separation and quantitation of Abm derivatives were achieved by HPLC with fluorescence detection. The calibration curve for Abm derivatives was linear over the concentration range of 2−100 (μL ml^{-1}) with a regression coefficient of 3.12 (mAU s ug^{-1} ml) and a correlation coefficient of 0.99 (See Figure S1 in the Supporting Information). Using the established HPLC methods, the loading properties of PVN^{Abm} were quantified as listed in Table 1. For the PVN^{Abm} formulated in phosphate buffer pH 7.5 with 20 mM EDTA (pore-open condition), there was approximately 37.2 μg of Abm loaded into 1 mg PVN^{Abm}. This equates to a loading capacity of ~177 Abm molecules per PVN. The loading efficiency, the percentage of Abm loaded in the virus nanoparticle with respect to the initial amount of Abm in loading formulation, was ~34.9%. To study the possibility of surface-bound Abm on viral capsids, the PVN^{Abm} was also formulated in the same buffer and pH value but without EDTA treatment. Our previous study of the PVN loading mechanism has confirmed that the pore-open condition is induced by the loss of Ca^{2+} and Mg^{2+} divalent ions via exposing RCNMV to EDTA chelating agent.[23] Therefore, any loading of Abm in the absence of EDTA could be considered as surface-bound molecules on the RCNMV capsid. The loading properties of PVN^{Abm} indicated that this surface association between Abm and RCNMV capsid was negligible as evident by the loading properties for the PVN^{Abm}-no EDTA formulation where only ~0.24 μg Abm was loaded in 1 mg PVN, which was equivalent to a loading capacity of less than 1 Abm molecule per PVN (Table 1). In the formulation of Dox-loaded PVN (PVN^{Dox}) for therapeutic drug delivery, a significant amount of Dox molecules were found to be surface-bound on the PVN^{Dox} surface due to the electrostatic interaction between the positively charged Dox and negatively charged protein residues of the RCNMV capsid surface.[23] However, in this study, the neutrally charged Abm molecules were not electrostatically attracted onto the capsid surface, but rather the entire loaded Abm would only infuse into the RCNMV capsid through the open pores on the capsid. The unchanged viral capsid's surface morphology of PVN^{Abm} also suggests the absence of surface-binding Abm on the viral capsid. Therefore, we infer that the loading capacity of ~177 Abm molecules per PVN were all encapsulated within the RCNMV capsid rather than surface binding on the capsid.

Table 1. Loading Properties of PVN^{Abm} Suspensions Formulated in Sodium Phosphate Buffer pH 7.5 with Different EDTA Concentrations

PVN^{Abm} formulations	Abm load[a] (μg)	loading capacity[b] (Abm/PVN)	loading efficiency[c] (%)
no/EDTA	0.24 ± 0.03	<1	
20 mM EDTA	37.2 ± 1.8	177 ± 9	34.9 ± 1.7

[a]Amount of Abm (μg) loaded in 1 mg PVN^{Abm}. [b]Load capacity reported as the number of Abm associated with each PVN capsid. [c]Load efficiency reported as the percentage of the Abm loaded to the initial amount of Abm used in preparation.

3.2. In vitro Release of Abm from PVN^{Abm}. The in vitro release performance of PVN^{Abm} was investigated in sodium acetate buffer pH 5.2 and M9 buffer pH 7.4 at room temperature. The pH values were selected to represent the acidic soil condition (pH 5.2) and the physiological condition of nematodes (pH 7.4). As shown in Figure 2a, 95% of free Abm diffused out of the dialysis bag within the first 5 h. In contrast, the rate of Abm release was considerably retarded by cargo encapsulation in RCNMV as only 24% and 28% of loaded Abm were released from PVN^{Abm} in pH 5.2 and pH 7.4 release buffers, respectively, within 5 h of exposure (Figure 2b). PVN^{Abm} exhibited a burst release of 16% loaded Abm in pH 7.4 release buffer within the first 1 h, then a gradual release of ~96% loaded Abm in the following 12 h. This burst release is related to the structural dynamics of RCNMV capsid as pH increases.[23] In pH 5.2 release buffer, no release of PVN^{Abm} was detected in the first 1 h but ~91% loaded Abm was still gradually released from PVN^{Abm} in 12 h with a slightly lower rate of release when compared with its release in pH 7.4 buffer. Almost complete release of all loaded Abm was achieved for PVN^{Abm} in both release buffers within 24 h. This is because the encapsulated Abm molecules were only physically entrapped by RCNMV capsid rather than electrostatically or chemically associated with RCNMV nucleic acids or capsid proteins. As a result, PVN^{Abm} displayed a fast and complete release of all encapsulated Abm because of the chemical potential gradient in the release study. In addition, the intact integrity of PVN^{Abm} at all release times was determined by agarose gel electrophoresis (see Figure S2 in Supporting Information).

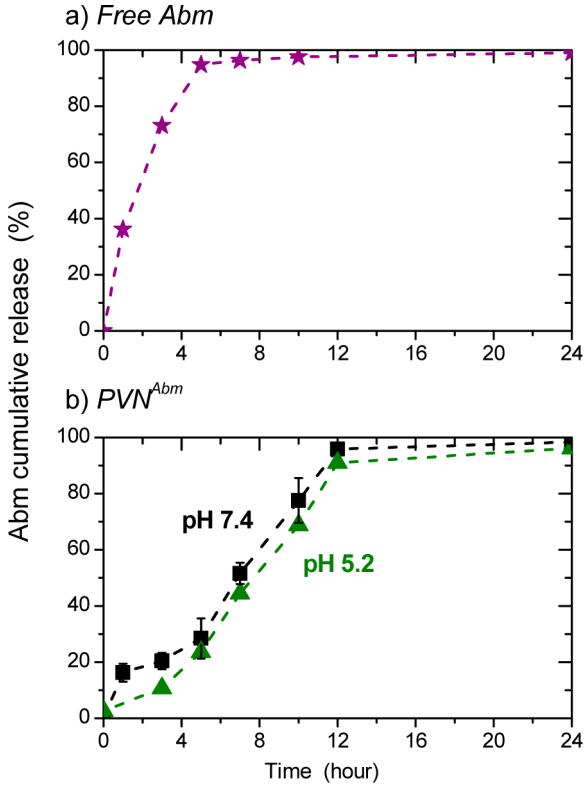

Figure 2. Cumulative Abm release over time for a) free Abm solution released in sodium acetate buffer pH 5.2 (magenta star) and (b) PVN^{Abm} suspension released in either sodium acetate buffer pH 5.2 (green triangle) or M9 buffer pH 7.4 (black square). The lines are guides for the eye.

3.3. Bioavailability of PVN^{Abm} to *C. elegans* Nematode. Bioavailability of PVN^{Abm} was evaluated utilizing *C. elegans* nematodes in liquid culture. Abm acts as a paralytic with exposed nematodes displaying a rigid, linear appearance and a characteristic loss of mobility (immobilized) versus the flexible

DOI: 10.1021/acsami.5b00940
ACS Appl. Mater. Interfaces 2015, 7, 9546−9553

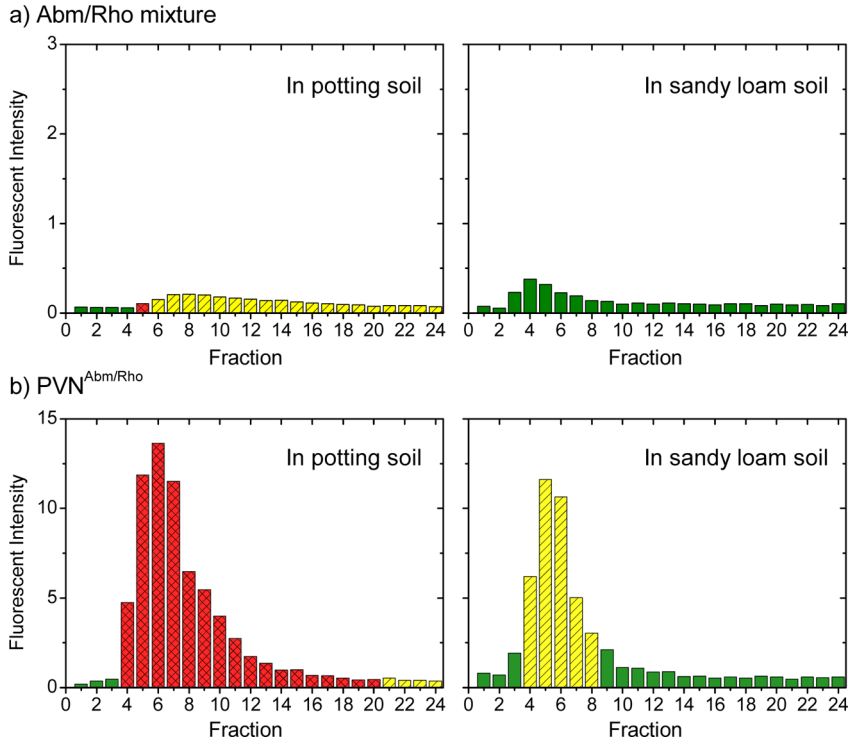

Figure 3. Characterization of soil mobility for (a) Abm/Rho mixture and (b) $PVN^{Abm/Rho}$ in the potting soil and sandy loam soil measured by eluting samples through the soils by 24 fractions of deionized water. The amount of sample in each efflux were assayed by fluorescence intensity of Rho molecules and the bioavailability of Abm molecules to cause *C. elegans* nematodes to be totally immobilized (red), impaired at 50% immobilized/50% mobilized (yellow), and totally mobilized (green).

form and undulating movement (mobilized) exhibited by untreated nematodes. LC_{50} values, defined as the concentration of Abm at which 50% nematodes were immobilized after 24 h of exposure, only showed a slight difference between the free Abm (LC_{50} of $1.5 \pm 0.4 \times 10^{-7}$ M) and PVN^{Abm} (LC_{50} of $1.3 \pm 0.6 \times 10^{-7}$ M). By a combination of the LC_{50} values and the in vitro release results where all the Abm was released from PVN^{Abm} in 24 h, it seems apparent that the released Abm from PVN^{Abm} retained the equivalent bioavailability to the *C. elegans* nematodes as free Abm.

3.4. Improved Soil Mobility of Abm by PVN Carrier. RCNMV were dual formulated with Abm and Rho to form the $PVN^{Abm/Rho}$ to track PVN's mobility through the soil via Rho's fluorescence. $PVN^{Abm/Rho}$ and free Abm/Rho were applied to a soil column containing either potting soil or sandy loam soil, and then eluted by addition of 24 aliquots of DI water. As shown in Figure 3a, the efflux of Abm/Rho mixture from the soil column presented low fluorescent intensity and low toxicity to nematodes; indicating that most of the free Abm/Rho compounds were retained in the soil column because of their poor mobility in both soil types, especially in sandy loam soil. The soil immobility of Abm was caused by its higher affinity to bind to organic compounds in the soil because of the hydrophobic/lipophilic nature of Abm.[12] In contrast, the efflux of $PVN^{Rho/Abm}$ shows a significant increase in the fluorescent intensity and nematode toxicity (Figure 3b) demonstrating that the PVN carrier mobilized its loading cargoes of Rho and Abm in both sandy loam soil and potting soil. While encapsulating Abm within PVN successfully enhanced the Abm's mobility in the soil, the degree of mobility was varied in the two tested soil types. This variability suggests that the surface chemistry of PVNs should be tuned for different soil types to achieve consistent mobility in the applications.

3.6. Enhanced Crop Protection in Soil by PVN^{Abm}. The nematicide efficacy of PVN^{Abm} and free Abm was tested with tomato seedlings that were planted in sandy loam soil infected with RKN. After 5 weeks of RKN inoculation, the crop protection results were evaluated by root growth and galling on roots on the basis of a 0−4 unit-scale. As listed in Table 2, the uninfected tomato seedlings as a negative control had a score of zero for both optimum root growth and no galling on the root (Figure 4a). In contrast, the positive infection control of RKN-infected plant had the worst score of 4 for both root growth and root galling because of reduced root growth and extensive galling knots on the root (Figure 4b). Application of free Abm

Table 2. Crop Protection Results of Abm and PVN^{Abm} to Tomato Seedlings Infected with *M. hapla* Root Knot Nematode (RKN) in Sandy Loam Soil under Greenhouse Conditions

		RKN-infected plant		
evaluation	uninfected plant	positive control	free Abm	PVN^{Abm}
root growth score[a]	0	4.0	3.0 (±0.3)	2.0 (±0.3)
root galling score[b]	0	4.0	3.7 (±0.4)	2.8 (±0.6)

[a]Plant root growth score was determined at 5 weeks after treatment, using a 0−4 unit scale where 0 = optimum growth of uninfected plant and 4 = worst root growth of the infected plant. [b]Plant root galling score determined at 5 weeks after treatment, obtained using a 0−4 unit scale where 0 = no galling of uninfected plants and 4 = worst galling of infected plants. Data were reported by means of five replications.

DOI: 10.1021/acsami.5b00940
ACS Appl. Mater. Interfaces 2015, 7, 9546−9553

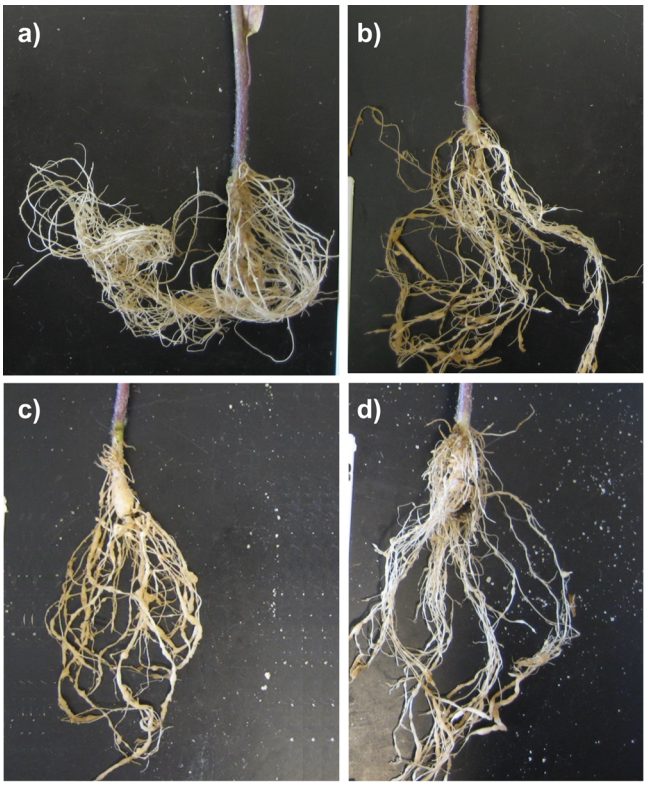

Figure 4. Evaluation of root system for (a) uninfected tomato seedling, (b) *M. hapla* root knot nematode (RKN) infected tomato seedling, (c) RKN-infected tomato seedlings treated with free Abm, and (d) RKN-infected tomato seedling treated with PVN^{Abm}. All plants were grown in a greenhouse for 5-weeks after treatment.

did not display an effective prevention of RKN damage as evident by a very slight improvement in root growth (score of 3.0) and root galling (score of 3.7) for the infected tomato seedlings (Table 2, Figure 4c). However, the PVN^{Abm} treatment exhibited a significant improvement in nematode control with a score of 2.0 for root growth and 2.8 for root galling for the infected tomato seedlings (Table 2, Figure 4d). Therefore, the increased soil mobility of Abm by PVN encapsulation demonstrated a very close correlation with the enhanced crop protection against RKN in the soil. PVN carrier not only addressed Abm's issue of soil immobility but also enabled a controlled released strategy for the bioavailability of Abm to nematodes during application. Although it was found that PVN^{Abm} treated plants displayed a reduced number of galling at the top portion of the plant roots, RKN infection still occurred toward the bottom portion of the roots (Figure 4d). This reduced efficacy in the lower portion of the roots could be caused by the limited mobility of PVN^{Abm} in sandy loam soil. To achieve complete protection, engineering the surface chemistry of PVN capsid to further increase its mobility in the soil would be necessary.

4. CONCLUSION

In this study, RCNMV-derived PVN technology was further exploited for the delivery of the nematicide Abm for PPN control. As a neutrally charged molecule, the loading of Abm within PVN resulted in a complete encapsulation within the viral capsid with a loading capacity of ~177 Abm molecules per PVN. The PVN^{Abm} addressed the lack of Abm mobility in soil and enabled a controlled release strategy for the bioavailability of Abm to nematodes during application. PVN^{Abm} exhibited the same bioavailability against *C. elegans* nematodes as free Abm in liquid culture but where free Abm cannot be adequately dispersed through soil, PVN^{Abm} possesses increased soil mobility as evident by its clearance through a soil column. This increase in soil mobility leads to the observed enhanced crop protection against RKN in the soil by PVN^{Abm} as compared to the same dose of free Abm. PVN^{Abm} enlarged the limited zone of protection against nematodes around the tomato seedling root system enabling the efficient delivery of Abm in the soil. The net result of treating with PVN^{Abm} versus Abm in nematode infested soil was healthier root growth and reduced number of gallings on the root of the infected tomato seedlings. Additional surface chemistry modifications of PVN^{Abm}, tailored to the soil type, could further increase the efficacy of nematode control in the bottom portion of the plant root by optimizing the movement of PVN in the tested soil and tuning the Abm release from PVN^{Abm}.

■ ASSOCIATED CONTENT

Supporting Information

HPLC chromatograms and calibration curve for quantitation of Abm in PVN^{Abm} (Figure S1) and agarose gel electrophoresis of PVN^{Abm} released in M9 buffer at different release times (Figure S2). The Supporting Information is available free of charge on the ACS Publications website at DOI: 10.1021/acsami.5b00940.

■ AUTHOR INFORMATION

Corresponding Author

*E-mail: jacrowe@ncsu.edu. Tel.: (+1) 971 2171079.

Notes

The authors declare no competing financial interest.

■ ACKNOWLEDGMENTS

This research was funded by a grant from the Bill & Melinda Gates Foundation (J.A.W. and S.A.L.) through the Grand Challenges Explorations initiative and USDA NIFA Agricultural System and Technology, Nanotechnology for Agricultural and Food System (S.A.L., J.A.W., T.L.S., and C.H.O.). We gratefully acknowledge their support. We would also like to thank the NC State University College of Textiles and College of Agricultural and Life Sciences' North Carolina Agricultural Research Station for providing their facility and support in this work.

■ REFERENCES

(1) Abad, P.; Gouzy, J.; Aury, J. M.; Castagnone-Sereno, P.; Danchin, E.; Perfus-Barbeoch, L.; Anthouard, V.; Artiguenave, F.; Blok, V. C.; Caillaud, M. C.; Coutinho, P. M.; Dasilva, C.; De Luca, F.; Deau, F.; Esquibet, M.; Flutre, T.; Goldstone, J. V.; Hamamouch, N.; Hewezi, T.; Jaillon, O.; Jubin, C.; Leonetti, P.; Magliano, M.; Majer, T. R.; Markov, G. V.; McVeigh, P.; Pesole, G.; Poulain, J.; Robinson-Rechavi, M.; Sallet, E.; Séqurens, B.; Steinbach, D.; Tytgat, T.; Ugarte, E.; van Ghelde, C.; Veronico, P.; Baum, T. J.; Blaxter, M.; Bleve-Zacheo, T.; Davis, E. L.; Ewbank, J. J.; Favery, B.; Grenier, E.; Henrissat, B.; Jones, J. T.; Laudet, V.; Maule, A. G.; Quesneville, H.; Rosso, M. N.; Schiex, T.; Smant, G.; Weissenbach, J.; Wincker, P. Genome Sequence of the Metazoan Plant-Parasitic Nematode Meloidogyne Incognita. *Nat. Biotechnol.* **2008**, *26*, 909−915.

(2) Sasser, J. Root-Knot Nematodes: A Global Menace to Crop Production. *Plant Dis.* **1980**, *64*, 36−41.

(3) Nusbaum, C. J.; Ferris, H. The Role of Cropping Systems in Nematode Population Management. *Annu. Rev. Phytopathol.* **1973**, *11*, 423−440.

DOI: 10.1021/acsami.5b00940
ACS Appl. Mater. Interfaces 2015, 7, 9546−9553

(4) Cook, R. Genetic Resistance to Nematodes: Where Is It Useful? *Australas. Plant Pathol.* **2004**, *33*, 139−150.
(5) Sikora, R.; Fernandez, E. In *Plant Parasitic Nematodes in Tropical and Subtropical Agriculture*, 2nd ed; Luc, M., Sikora, R., Bridge, J., Eds.; CABI Publishing: Wallingford, U.K., 2005; pp 319−392.
(6) Global Nematicide Market: Market Analysis and Opportunites. *Agriculture/Specialty Pesticides*, 3rd ed; Kline & Company: Winter Haven, FL, 2012.
(7) World Agricultural Pesticides Market. *Freedonia*, **2012**, 458.
(8) Santos, B. M.; Gilreath, J. P.; Motis, T. N.; Noling, J. W.; Jones, J. P.; Norton, J. A. Comparing Methyl Bromide Alternatives for Soilborne Disease, Nematode and Weed Management in Fresh Market Tomato. *Crop Prot.* **2006**, *25*, 690−695.
(9) Stirling, A. M.; Stirling, G. R.; Macrae, I. C. Microbial Degradation of Fenamiphos after Repeated Application to a Tomato-Growing Soil. *Nematologica* **1992**, *38*, 245−254.
(10) Putter, I.; Mac Connell, J. G.; Preiser, F. A.; Haidri, A. A.; Ristich, S. S.; Dybas, R. A. Avermectins: Novel Insecticides, Acaricides and Nematicides from a Soil Microorganism. *Experientia* **1981**, *37*, 963−964.
(11) Holden-Dye, L.; Walker, R. J. *WormBook* **2007**, DOI: 10.1895/wormbook.1.143.1.
(12) Krogh, K. A.; Søeborg, T.; Brodin, B.; Halling-Sørensen, B. Sorption and Mobility of Ivermectin in Different Soils. *J. Environ. Qual.* **2008**, *37*, 2202−2211.
(13) Gruber, V. F.; Halley, B. A.; Hwang, S. C.; Ku, C. C. Mobility of Avermectin B1a in Soil. *J. Agric. Food Chem.* **1990**, *38*, 886−890.
(14) Cooper, A.; Oldinski, A.; Ma, H.; Bryers, J. D.; Zhang, M. Chitosan-Based Nanofibrous Membranes for Antbacterial Filter Applications. *Carbohydr. Polym.* **2013**, *92*, 254−259.
(15) Cabrera, J. A.; Menjivar, R. D.; Dababat, A. e.-F. A.; Sikora, R. A. Properties and Nematicide Performance of Avermectins. *J. Phytopathol.* **2013**, *161*, 65−69.
(16) Chukwudebe, A. C.; Feely, W. F.; Burnett, T. J.; Crouch, L. S.; Wislocki, P. G. Uptake of Emamectin Benzoate Residues from Soil by Rotational Crops. *J. Agric. Food Chem.* **1996**, *44*, 4015−4021.
(17) Mrozik, H. In *Natural and Engineered Pest Management Agents*; Hedin, P. A, Menn, J. J., Hollingworth, R. M., Eds.; American Chemical Society: Washington, DC, 1993; pp 5473.
(18) Fan, T.; Feng, J.; Ma, C.; Yu, C.; Li, J.; Wu, X. Preparation and Characterization of Porous Micropheres and Application in Controlled-Release of Abamectin in Water and Soil. *J. Porous Mater.* **2014**, *21*, 113−119.
(19) Demchak, R. J.; Dybas, R. A. Photostability of Abamectin/zein Microspheres. *J. Agric. Food Chem.* **1997**, *45*, 260−262.
(20) Wang, L. L.; Wang, Z.; Zhang, B. H.; Xiao, K. F. Study on Preparation of Abamectin Microcapule with Interfacial Polymerization. *Adv. Mater. Res.* **2013**, 1090−1094.
(21) Basnayake, V. R.; Sit, T. L.; Lommel, S. A. The Genomic RNA Packaging Scheme of Red Clover Necrotic Mosaic Virus. *Virology* **2006**, *345*, 532−539.
(22) Sherman, M. B.; Guenther, R. H.; Tama, F.; Sit, T. L.; Brooks, C. L.; Mikhailov, A. M.; Orlova, E. V.; Baker, T. S.; Lommel, S. A. Removal of Divalent Cations Induces Structural Transitions in Red Clover Necrotic Mosaic Virus, Revealing a Potential Mechanism for RNA Release. *J. Virol.* **2006**, *80*, 10395−10406.
(23) Cao, J.; Guenther, R. H.; Tim, T. L.; Opperman, C. H.; Lommel, S. A.; Willoughby, J. A. Loading and release mechanism of RCNMV derived plant viral nanoparticle for drug delivery of doxorubicin. *Small* **2014**, *10*, 5126−5136.
(24) Franzen, S.; Lommel, S. A. Targeting Cancer with "Smart Bombs": Equipping Plant Virus Nanoparticles for a "Seek and Destroy" Mission. *Nanomedicine (London, U. K.)* **2009**, *4*, 575−588.
(25) Loo, L.; Guenther, R. H.; Lommel, S. A.; Franzen, S. Infusion of Dye Molecules into Red Clover Necrotic Mosaic Virus. *Chem. Commun. (Cambridge, U. K.)* **2008**, 88−90.
(26) Lockney, D.; Franzen, S.; Lommel, S. Viruses as Nanomaterials for Drug Delivery. *Methods Mol. Biol.* **2011**, *726*, 207−221.
(27) Lockney, D. M.; Guenther, R. N.; Loo, L.; Overton, W.; Antonelli, R.; Clark, J.; Hu, M.; Lommel, S. A.; Franzer, S. The Red Clover Necrotic Mosaic Virus Capsid as a Multifunctional Cell Targeting Plant Viral Nanoparticle. *Bioconjugate Chem.* **2011**, *22*, 67−73.
(28) Honarbakhsh, S.; Guenther, R. H.; Willoughby, J. A.; Lommel, S. A.; Pourdeyhimi, B. Polymeric Systems Incorporating Plant Viral Nanoparticle for Tailored Released of Therapuetics. *Adv. Healthcare Mater.* **2013**, *2*, 1001−1007.
(29) Xiong, Z. G.; Lommel, S. A. Red Clover Necrotic Mosaic Virus Infectious Transcripts Synthesized in Vitro. *Virology* **1991**, *182*, 388−392.
(30) *Zetasizer Series: Dynamic Light Scattering and Zeta Potential*; Malvern Instruments: Malvern, U.K., 2012.
(31) *OECD Test No. 312: Leaching in Soil Columns*; OECD Publishing: Paris, 2004.
(32) Opperman, C. H.; Chang, S. Effects of Aldicarb and Fenamiphos on Acetycholinesterase and Motility of Caenorhabditis Elegans. *J. Nematol.* **1991**, *23*, 20−27.
(33) Payne, L. D.; Hicks, M. B.; Wehner, T. A. Determination of Abamectin and/or Ivermectin in Cattle Feces at Low Parts Per Billion Levels Using HPLC with Fluorescence Detection. *J. Agric. Food Chem.* **1995**, *43*, 1233−1237.
(34) Tolan, J. W.; Eskola, P.; Fink, D. W.; Mrozik, H.; Zimmerman, L. A. Determination of Avermectins in Plasma at Nanogram Levels Using High-Performance Liquid Chromatography with Flourescence Detection. *J. Chromatogr.* **1980**, *190*, 367−376.

DOI: 10.1021/acsami.5b00940
ACS Appl. Mater. Interfaces 2015, 7, 9546−9553